

Exactly solvable model behind Bose-Hubbard dimers, Ince-Gauss beams, and aberrated optical cavities

R. Gutiérrez-Cuevas,^{1,2,*} D. H. J. O'Dell,^{3,†} M. R. Dennis,^{4,‡} and M. A. Alonso^{2,5,6,§}

¹*Institut Langevin, ESPCI Paris, Université PSL, CNRS, 75005 Paris, France*

²*Aix Marseille Univ, CNRS, Centrale Marseille,*

Institut Fresnel, UMR 7249, 13397 Marseille Cedex 20, France

³*Department of Physics and Astronomy, McMaster University,
1280 Main St. W., Hamilton, Ontario, L8S 4M1, Canada*

⁴*School of Physics and Astronomy, University of Birmingham, Birmingham B15 2TT, UK*

⁵*The Institute of Optics, University of Rochester, Rochester, NY 14627, USA*

⁶*Laboratory for Laser Energetics, University of Rochester, Rochester, NY 14627, USA*

(Dated: May 29, 2023)

By studying the effects of quadratic anisotropy and quartic perturbations on the two-dimensional harmonic oscillator, one arrives at a simple model termed here the Ince oscillator, whose analytic solutions are given in terms of Ince polynomials. This one model unifies diverse physical systems, including aberrated optical cavities that are shown to support Ince-Gauss beams as their modes, and the two-mode Bose-Hubbard dimer describing two coupled superfluids. The Ince oscillator model describes a topological transition which can have very different origins: in the optical case, which is fundamentally linear, it is driven by the ratio of astigmatic to spherical mirror aberrations, whereas in the superfluid case it is driven by the ratio of particle tunneling to interparticle interactions and corresponds to macroscopic quantum self trapping.

Introduction. Analogies between physical phenomena arise when, in certain limits, their different fundamental equations reduce to similar models. A very basic model is the harmonic oscillator (HO), which in both path/classical or wave/quantum forms describes a variety of phenomena in mechanics and optics [1, 2]. The isotropic 2-dimensional HO (2DHO) is more striking, since it possesses a hidden SU(2) symmetry that endows it with three constants of the motion (CoMs) involving its position and momentum. For the classical case these constants take the form

$$L_j \equiv \frac{1}{4} \left(\frac{\mathbf{q}}{\sqrt{\gamma}} - i\sqrt{\gamma}\mathbf{p} \right) \sigma_j \left(\frac{\mathbf{q}}{\sqrt{\gamma}} + i\sqrt{\gamma}\mathbf{p} \right), \quad (1)$$

for $j = 1, 2, 3$, where $\mathbf{q} = (q_x, q_y)$ is the position, $\mathbf{p} = (p_x, p_y)$ is the momentum, γ is a positive constant with the appropriate units for the problem in question, and σ_j are the (permuted) Pauli matrices

$$\sigma_1 = \begin{pmatrix} 1 & 0 \\ 0 & -1 \end{pmatrix}, \quad \sigma_2 = \begin{pmatrix} 0 & 1 \\ 1 & 0 \end{pmatrix}, \quad \sigma_3 = \begin{pmatrix} 0 & -i \\ i & 0 \end{pmatrix}. \quad (2)$$

Note that $L_1^2 + L_2^2 + L_3^2 = (\frac{1}{4\gamma}q^2 + \frac{\gamma}{4}p^2)^2$ is proportional to the Hamiltonian squared, where $q^2 = \mathbf{q} \cdot \mathbf{q}$ and $p^2 = \mathbf{p} \cdot \mathbf{p}$. The Poisson brackets (or the commutators in the quantum case) of the CoMs resemble angular momentum algebra. Of these CoMs, L_1 and L_2 are quadratic in both \mathbf{p} and \mathbf{q} , but $L_3 = (q_x p_y - q_y p_x)/2$ [half the orbital angular momentum (OAM)] is linear in both \mathbf{p} and \mathbf{q} , the linearity in \mathbf{p} playing a central role in what follows.

Here, we present an analytically solvable, nonlinear model we call the *Ince oscillator* based on the quantum 2DHO experiencing a perturbation whose effect is

described by the Ince operator $\hat{\mathcal{I}}$, defined as

$$\hat{\mathcal{I}} = \frac{\alpha}{2} \hat{L}_1 + \hat{L}_3^2, \quad (3)$$

where \hat{L}_j are the Fradkin-Stokes operators corresponding to the SU(2) CoMs, and α is a positive parameter. This system can be visualized physically as a 2DHO subject to the two simplest meaningful perturbations: quadratic asymmetry and a quartic correction to the potential (determined by \hat{L}_1 and \hat{L}_3^2 respectively). It can then be considered as the simplest generalization of a 2DHO that not only presents topological transitions, but can also be solved analytically, in terms of Ince polynomials [3, 4]. This simplicity endows it with an important level of universality, so that it describes a range of different physical systems. We emphasize two such systems for which the connection is particularly surprising. The first is a linear, optical resonant cavity like those used in lasers and high-precision interferometers [5, 6]. In the presence of small amounts of simple aberrations, the cavity modes are shown to correspond to Ince-Gauss (IG) beams, which have received significant attention recently [3, 4, 7–14]. The second system is the Bose-Hubbard (BH) dimer model [15–26], a workhorse in condensed matter physics providing a minimal model for coupled reservoirs of superfluid helium [27, 28], coupled atomic Bose-Einstein condensates (BECs) [29–35], and coupled polariton BECs in semiconductor microcavities [36, 37], among others.

2D harmonic oscillator. The 2DHO obeys the Schrödinger equation $i\eta \partial_\tau |\psi\rangle = \hat{H}_0 |\psi\rangle$, where η is a constant (e.g. the reduced Planck constant for mechanics or the reduced wavelength for optics), τ is the propaga-

tion/evolution parameter, and \hat{H}_0 is the Hamiltonian

$$\hat{H}_0 = \frac{\kappa}{2} \left(\frac{1}{\gamma} \hat{q}^2 + \gamma \hat{p}^2 \right), \quad (4)$$

where κ is also a constant with appropriate units for the problem in question. In the position representation, $\hat{\mathbf{q}} \rightarrow (q_x, q_y)$ and $\hat{\mathbf{p}} \rightarrow -i\eta(\partial_{q_x}, \partial_{q_y})$. The eigenvalues of the Hamiltonian in Eq. (4) are $\kappa\eta(N+1)$, where N is a non-negative integer referred to as the total order. There are $N+1$ degenerate eigenstates of \hat{H}_0 for any N , so the choice of a set of eigenfunctions is not unique [1, 38], and different eigenstates are obtained through separation of variables in several ways [7, 8]. For example, separation in Cartesian coordinates leads to Hermite-Gauss (HG) modes, while separation in polar coordinates gives Laguerre-Gauss (LG) modes [2].

Schwinger's coupled oscillator model [1] provides an elegant description of the 2DHO, based on the Fradkin-Stokes operators $\hat{\mathbf{L}} \equiv (\hat{L}_1, \hat{L}_2, \hat{L}_3)$, which satisfy the $\mathfrak{su}(2)$ commutation relations $[\hat{L}_i, \hat{L}_j] = i\eta \sum_k \epsilon_{ijk} \hat{L}_k$, with ϵ_{ijk} being the Levi-Civita tensor. These operators commute with the unperturbed Hamiltonian $[\hat{H}_0, \hat{L}_j] = 0$ since

$$\hat{\mathbf{L}} \cdot \hat{\mathbf{L}} = \hat{L}_1^2 + \hat{L}_2^2 + \hat{L}_3^2 = \frac{1}{4\kappa^2} \hat{H}_0^2 - \frac{\eta^2}{4}. \quad (5)$$

Thus, the degenerate set of modes of \hat{H}_0 with equal N can be mapped onto a collective spin with total angular momentum $N/2$ [38–42]. Different spin axes correspond to different modes [38–40]: the HG and LG modes are eigenstates of \hat{L}_1 and \hat{L}_3 , respectively.

Perturbed 2DHO. The degeneracy of the 2DHO can be removed by adding a small perturbation \hat{W} to the Hamiltonian:

$$\hat{H} = \hat{H}_0 + \hat{W}(\hat{\mathbf{q}}, \hat{\mathbf{p}}), \quad (6)$$

Propagation/evolution over an interval τ is described by the operator $\exp(-i\tau\hat{H}/\eta) = \exp[-i\tau(\hat{H}_0 + \hat{W})/\eta]$. Since \hat{W} is small, we can use the first Born approximation to arrive at

$$\exp(-i\tau\hat{H}/\eta) = \exp(-i\tau\hat{H}_0/\eta) \left(1 - \frac{i\tau}{\eta} \hat{W} \right), \quad (7)$$

where

$$\hat{W} = \frac{1}{\tau} \int_0^\tau d\tau' \exp\left(\frac{i\tau'}{\eta} \hat{H}_0\right) \hat{W}(\hat{\mathbf{q}}, \hat{\mathbf{p}}) \exp\left(-\frac{i\tau'}{\eta} \hat{H}_0\right). \quad (8)$$

By assuming that τ is much larger than the oscillation period, changing variables to $\kappa\tau' = \theta$, and using the canonical commutation relation, we can write this operator as

$$\hat{W} \approx \frac{1}{2\pi} \int_0^{2\pi} d\theta \hat{W} \left(\hat{\mathbf{q}} \cos \theta + \gamma \hat{\mathbf{p}} \sin \theta, \hat{\mathbf{p}} \cos \theta - \hat{\mathbf{q}} \frac{\sin \theta}{\gamma} \right). \quad (9)$$

The operator $\hat{\mathcal{P}}$ is then simply the accumulation of the effect of \hat{W} over many cycles. This accumulation has the effect of making $\hat{\mathcal{P}}$ symmetric in $\hat{\mathbf{q}}$ and $\hat{\mathbf{p}}$, so that it commutes with the unperturbed Hamiltonian \hat{H}_0 . Since we are in the perturbative regime, the modes must then be eigenstates of both \hat{H}_0 and $\hat{\mathcal{P}}$.

We consider simple forms for \hat{W} , corresponding to low-order polynomials in position and momentum. It is easy to show that Eq. (9) vanishes for any odd-order monomial, so it is sufficient to consider even powers. Since we consider simple physical systems where the kinetic and potential parts are separate, we focus on even-order monomials that include either $\hat{\mathbf{q}}$ or $\hat{\mathbf{p}}$.

Ince oscillator. We define the Ince oscillator as a 2DHO subject to the two simplest perturbations: an anisotropic quadratic and a rotationally symmetric quartic terms. Therefore, we set

$$\hat{W} = \frac{\epsilon_1}{2\gamma} (\hat{q}_y^2 - \hat{q}_x^2) + \frac{\epsilon_2 \hat{q}^4}{\gamma^2} \quad (10)$$

where the coefficients ϵ_1 and ϵ_2 are assumed to be small, justifying the perturbative approach. This leads to

$$\hat{\mathcal{P}} = 2\epsilon_2 \left(\frac{3}{4\kappa^2} \hat{H}_0^2 + \frac{\eta^2}{4} - \hat{\mathcal{I}} \right). \quad (11)$$

where $\hat{\mathcal{I}}$ is the Ince operator defined in Eq. (3), with $\alpha/\eta = \epsilon_1/\eta\epsilon_2$ being a dimensionless parameter that can take any real value. Note that if we had replaced the position operators in Eq. (10) with the corresponding momentum operators (with the appropriate factors of γ for dimensional reasons) the result would have been the same. In particular, a quartic perturbation in momentum would correspond to a relativistic correction for quantum-mechanical particle evolution or a postparaxial correction for monochromatic optical propagation.

The two terms in the perturbation each break the degeneracy in a different way, hence selecting a specific set of modes: HG modes (separable in Cartesian coordinates) are eigenstates of \hat{L}_1 so they are selected by quadratic asymmetry ($\alpha/\eta \rightarrow \infty$), while LG modes (separable in polar coordinates) are eigenstates of \hat{L}_3 and are hence selected by a rotationally-symmetric quartic perturbation ($\alpha/\eta = 0$). Since $\hat{\mathcal{P}}$ is quadratic in \hat{L}_3 , some degeneracy remains in this case between LG modes with the same amplitude profile but opposite OAM.

For an eigenstate of \hat{H}_0 to also be an eigenstate of $\hat{\mathcal{P}}$, it is sufficient that it be an eigenstate of $\hat{\mathcal{I}}$:

$$\hat{\mathcal{I}} |\psi_{N,\mu}^{(p)}(\alpha)\rangle = \frac{\eta^2 a_{N,\mu}^{(p)}}{4} |\psi_{N,\mu}^{(p)}(\alpha)\rangle, \quad (12)$$

where each mode is identified by its total order N , parity p , and index μ , ordered such that the corresponding eigenvalues satisfy $a_{N,\mu}^{(p)} < a_{N,\mu+2}^{(p)}$ and $a_{N,\mu}^{(o)} < a_{N,\mu}^{(e)}$. As

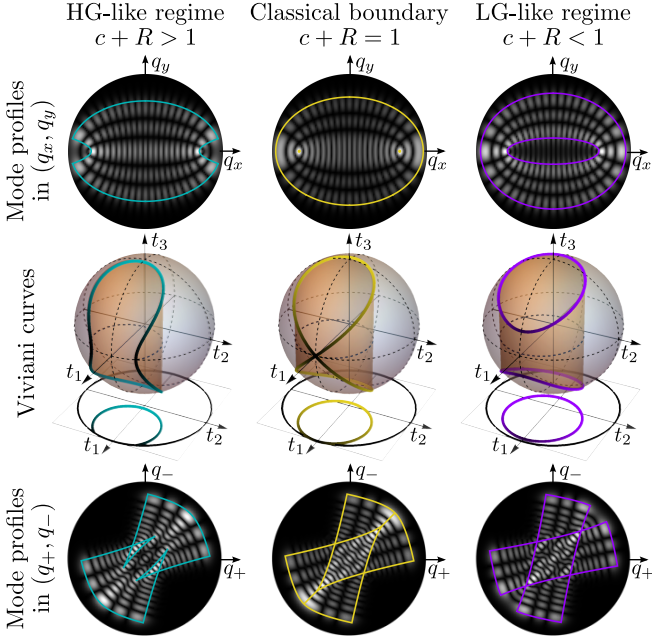


FIG. 1. Various representations of the topological transition in the classical limit for the same even IG mode with $N = 22$ and $\mu = 18$. The left and right columns correspond, respectively, to the two topologically distinct regimes: HG-like (turquoise), and LG-like (purple); the middle column shows the boundary between them (yellow). The first row depicts $|\langle \mathbf{q} | \psi_{N,\mu}^{(p)}(\alpha) \rangle|$ (corresponding, e.g., to the transverse profile of an IG beam) and whose significant values are contained within the caustics, indicated by the overlaid color curves. The second row shows the generalized Viviani curves on the Bloch/Poincaré sphere. The third row shows $|\langle q_+, q_- | \psi_{N,\mu}^{(p)}(\alpha) \rangle|$, the amplitude over the real parts of the quadratures of two modes in a BH dimer, as well as the corresponding caustics. Note that $\langle q_+, q_- | \psi_{N,\mu}^{(p)}(\alpha) \rangle$ can be calculated from $\langle \mathbf{q} | \psi_{N,\mu}^{(p)}(\alpha) \rangle$ by Fourier transforming the latter in q_y and rotating the result by $\pi/4$.

discussed in the Supplemental Material [43], these eigenstates are the IG modes [3, 4, 7–10], which in the position representation are separable in elliptical coordinates with focal separation equal to $2(\alpha\gamma)^{1/2}$. The dependence on each variable is a combination of an exponential and an Ince polynomial. The spatial profile $|\langle \mathbf{q} | \psi_{N,\mu}^{(p)}(\alpha) \rangle|$ of some of these modes is shown in Fig. 1. This profile depends on α : for $\alpha/\eta \rightarrow \infty$ the modes reduce to HG modes, while for $\alpha/\eta \rightarrow 0$ they reduce to *real* LG modes (the superposition in equal amounts of two LG modes of equal radial profile and opposite vorticity). For intermediate values of α the modes resemble deformed versions of either HG or real LG modes; we refer to these as the HG-like and LG-like regimes, respectively. We emphasize that although our derivation of the equations defining the Ince oscillator involves perturbation theory, our treatment of the Ince operator itself [Eq. (12)] is exact.

Classical limit. In order to better understand the

two regimes for the IG modes and the transition between them, consider the “classical” limit (valid for large N) obtained by replacing the operators with c-number quantities. The classical version of Eq. (5) can be written as $t_1^2 + t_2^2 + t_3^2 = 1$, where $t_j = 2L_j/(\eta(N+1))$. This relation defines a unit Poincaré/Bloch sphere in the space $\mathbf{t} = (t_1, t_2, t_3)$. However, the modes must also be eigenstates of the Ince operator. The classical version of Eq. (12) can be written as

$$t_3^2 + \alpha t_1/\eta(N+1) = a/(N+1)^2, \quad (13)$$

where a is the eigenvalue. This equation corresponds to a parabolic cylinder in the space of \mathbf{t} . The mode can then be represented by the intersection of the unit sphere and this parabolic cylinder. This intersection is equivalent [26] to that of the sphere with the vertical cylinder $(t_1 - c)^2 + t_2^2 = R^2$, aligned along the t_3 axis, centered at $c = \alpha/2\eta(N+1)$ and of radius $R = \{1 + [(\alpha/2\eta)^2 - a]/(N+1)^2\}^{1/2}$ as shown in Fig. 1. These curves correspond to generalized Viviani curves, also known as Euclid spherical ellipses.

The generalized Viviani curves present two topologically distinct regimes, each linked to a type of IG mode. When $c + R > 1$ (left-hand column of Fig. 1), the intersection of the sphere and the cylinder is composed of a single loop. The projection of this intersection onto the (t_1, t_2) plane is an open circular segment that can be used to determine the caustics of the mode [39, 63], which tend to coincide with the inflection points of the mode’s amplitude at the edges of the areas occupied by the modes. In this case, the caustics take the shape of a curvilinear quadrangle composed of two sections of an ellipse and a section of each of the two branches of a confocal hyperbola. This shape mimics the profile of the HG-like mode. On the other hand, when $c + R < 1$ (right-hand column of Fig. 1) the intersection between the cylinder and the sphere is composed of two loops, both of which project onto a closed circle in the (t_1, t_2) plane, from which the caustics can be found to be two complete confocal ellipses, so that the mode resembles an elongated real LG mode. The boundary case $c + R = 1$ (middle column of Fig. 1), where the topological transition takes place, corresponds to a figure of eight-shaped curve (the original Viviani curve being a special case).

The topological transition is not only manifested in the shape of the eigenmodes, but also in the near-degeneracy of the corresponding eigenvalues as shown in Fig. 2. In the semiclassical limit, the eigenvalues can be determined through self-consistency conditions in the wave estimates [21, 23, 25, 41, 63–68] in which the solid angle enclosed by each loop of the generalized Viviani curves must be quantized as an odd multiple of $2\pi/(N+1)$ [63]. This quantization is related to a geometric phase through the Pancharatnam-Berry connection [41, 69–71]. In the HG-like regime, where the curve consists of only one loop, the total subtended solid angle must be an odd multiple of

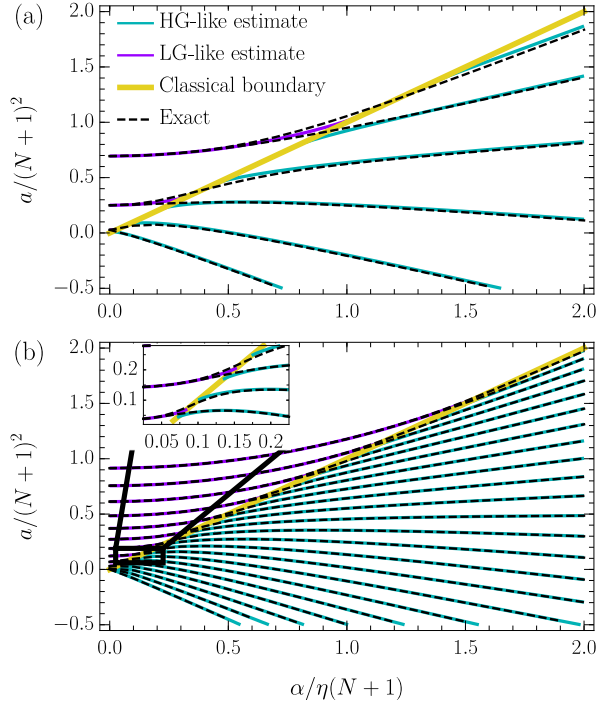


FIG. 2. Semiclassical and exact eigenvalues for the IG modes with (a) $N = 5$ and (b) $N = 22$, as functions of α .

$2\pi/(N+1)$, but in the LG-like regime, where the curve is composed of two loops, each loop must satisfy this condition so the total solid angle must be an even multiple of $2\pi/(N+1)$. This discrepancy creates a discontinuity at the topological transition at which the semiclassical estimate fails, as shown in Fig. 2. Away from the transition, the semiclassical estimate for the eigenvalue in Eq. (12) is nearly indistinguishable from the exact eigenvalue, even for small N .

Optical cavities. The first physical realization of the Ince oscillator discussed here is a linear (non-interacting) system corresponding to an aberrated optical cavity. Optical cavities are a central component of laser systems, and their shape determines the transverse profile of the generated beam [2, 72]. Cavities are also used in high-precision interferometric measurements [5]. These applications have motivated studies of the effect of optical aberrations [73] on the cavity modes. For instance, particular structured modes have been shown to be resilient to small amounts of aberrations in the cavities used for interferometric gravitational wave detection [6], and non-planar cavities have been used to produce Laughlin light states [74, 75]. However, very few cases lead to solutions in terms of simple closed-form expressions.

In the paraxial regime, a resonant cavity composed of two identical unaberrated curved mirrors can be mapped onto a 2DHO [2, 7, 8, 38, 39, 41]. The cavity is perturbed if the mirrors present slight aberrations that deform the wavefront after each reflection. Two of the simplest op-

tical aberrations are (Fig. 3): astigmatism, introduced by a deviation from rotational symmetry in the shape of the mirrors or by a slight misalignment of the system; and spherical aberration, which is a quartic deviation of the mirror's ideal radial shape. (A small deviation from paraxiality has a similar effect as spherical aberration.) A slight difference between the 2DHO and the cavity is that for the latter both the main quadratic potential and the aberrations act discretely each time the beam is reflected by the mirrors. However, it is shown in the Supplemental Material [43] that for a stable non-confocal cavity with a high quality factor, an averaging effect like that in Eq. (9) takes place so that the resulting modes are eigenstates not only of \hat{H}_0 but also of $\hat{\mathcal{L}}$, where now α quantifies the ratio between astigmatism and spherical aberration. They are therefore IG modes, which resemble HG modes when astigmatism dominates ($\alpha/\eta \rightarrow \infty$) and LG modes when spherical aberration dominates ($\alpha/\eta \rightarrow 0$). When propagating outside the cavity, IG modes are referred to as IG beams, whose applications have included micro-manipulation [14], encoding of quantum information [12, 13], and studies of vortex breakup [76]. It has been observed experimentally that IG beams result from resonators with slightly tilted or shifted mirrors [11], and earlier theoretical and experimental studies of imperfect optical cavities (without the use of the paraxial approximation) [77] found modes whose transverse profiles in retrospect resemble those of IG modes. The analysis presented here provides a rigorous foundation for this connection, where a clear relation is given between the parameters for the shape of the IG mode and those of the cavity.

BH dimer. Let us now consider the second-quantized form of the Fradkin-Stokes operators in terms of the annihilation operators $\hat{a}_j = (\hat{q}_j + i\hat{p}_j)/2^{1/2}$ with $j = x, y$ (setting $\eta = \gamma = 1$ for simplicity), and perform the canonical transformation $\hat{a}_{\pm} = (\hat{a}_x \mp i\hat{a}_y)/2^{1/2}$. The Ince operator can then be identified with the two-mode BH Hamiltonian, where $\hat{L}_1 = (\hat{a}_+^\dagger \hat{a}_- + \hat{a}_+ \hat{a}_-^\dagger)/2$ describes particle hopping and $\hat{L}_3 = (\hat{a}_+^\dagger \hat{a}_+ - \hat{a}_-^\dagger \hat{a}_-)/2$ describes the particle number difference between the two modes. The term with \hat{L}_3^2 accounts for on-site particle-particle interactions. Here, α controls the behavior of the system [19, 20] by fixing the ratio between the hopping and the interactions, and N corresponds to the total number of particles in the system. When $N \ll \alpha/\eta$ (the Rabi regime) particles can hop freely between sites, while in the opposite limit $\alpha/\eta \ll 1/N$ (the Fock regime) the population difference is locked by strong interactions, a phenomenon known as macroscopic quantum self trapping (MQST) [17] which is a manifestation of the topological transition on the Bloch sphere (see the Supplemental material [43] for more information about the BH dimer). Due to the canonical transformation, the two modes of the BH dimer do not correspond to the modes of the coor-

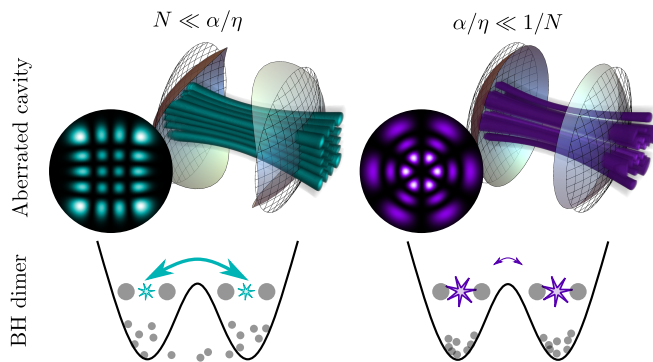


FIG. 3. Physical realizations. Top row: IG modes of total order N supported by an optical cavity with small amounts of astigmatism and spherical aberration, where the round insets show the transverse intensity profiles; Bottom row: representation of the BH dimer model as a BEC with N particles in a double well potential subject to on-site interactions (represented by stars) and hopping (represented by double arrows). For the BH dimer α represents the ratio between the two types of interaction, while for the IG modes it is the ratio between the two types of aberration in the cavity. Each system is depicted for values of the parameters well into one of the two regimes: (turquoise) Rabi/HG-like regime where hopping/astigmatism dominate, and (purple) Fock/LG-like regime where on-site interactions/spherical aberration dominate. The figure depicts the case of $N = 7$, even, $\mu = 3$, (left) $\alpha/\eta = 5N$, and (right) $\alpha/\eta = 1/5N$.

ordinates axes of the 2DHO, but rather to the two modes defining the sign of the OAM of the 2DHO. Additionally, the particle number difference between the two modes of the BH dimer corresponds to the net OAM in the Ince oscillator. It is then possible to write the representation of the wavefunction in terms of the real parts of the quadratures for each site from the corresponding IG modes, namely $\langle q_+, q_- | \psi_{N,\mu}^{(p)}(\alpha) \rangle$, by applying the operators $\exp(-i\pi\hat{L}_3/2\eta) \exp(i\pi\hat{L}_1/2\eta)$ to the spatial modes $\langle \mathbf{q} | \psi_{N,\mu}^{(p)}(\alpha) \rangle$. These two unitary operations are rotations of the Bloch sphere, which in coordinate space correspond to an antisymmetric fractional Fourier transform followed by a physical rotation [38]. Thus, the eigenstates of the BH dimer can be written as closed-form solutions of the Ince oscillator. An example of one of these wavefunctions and the corresponding caustics, calculated from the projection of the curve onto the (t_1, t_3) plane [39, 63], are shown in Fig. 1. These naturally two-dimensional solutions form a complete orthogonal basis that avoids the subtle issues associated with other approaches to the BH dimer such as the Bargmann state representation which is over complete [18, 78–81].

Conclusions and outlook. We have shown that the Ince oscillator, namely a 2DHO subject to anisotropic and quartic perturbations, corresponds to several apparently unrelated physical systems. Examples of such systems not treated explicitly here include the modes of slightly

anisotropic gradient index waveguides, bundles of coupled waveguides [82], and the evolution of polarization in a birefringent nonlinear medium [83]. Here we focused on two systems: an aberrated optical cavity and the BH dimer. We showed that the aberrated optical cavity has eigenmodes that are separable in elliptical coordinates, which correspond to the IG beams that have been widely used in structured light applications [3, 4, 7–14]. The classical analysis shows why there are two regimes for these modes, and explains the geometry of each. Furthermore, identifying the BH dimer as an Ince oscillator shows that the Ince polynomials are analytic representations of its eigenstates, a fact that has thus far been overlooked. It also shows that any system describable by the Ince oscillator shows the same rich dynamics as the bosonic Josephson junction, including analogues of plasma oscillations, pi-oscillations and macroscopic quantum self trapping.

The Ince oscillator and its modes have connections yet to be explored to several other physical systems, including the planar quantum pendulum and the Razavy potential [84, 85]. Moreover, the classical limit of this model leads to even more connections not treated here, such as the non-rigid pendulum [16], the simple pendulum [26], and the rotational dynamics of celestial bodies [86, 87].

A number of possible extensions can be considered. The effect of other perturbations, such as quartic astigmatism, can be studied with the expectation that it would lead to other implementations of the BH dimer and its generalizations. In particular, a slow rotation of the 2DHO would induce a perturbative term proportional to \hat{L}_3 , which would allow modeling nonplanar ring cavities and unbalanced (tilted) BH dimers. Another interesting generalization is the effect of perturbations in the 3DHO where there are even more separable families of solutions, leading to a model for the more complex dynamics of the three-site BH system [88–90]. These connections and extensions will be explored in future work.

The authors acknowledge J.M. Fellows for useful suggestions. The work by R.G.C. and M.A.A. was supported by the Excellence Initiative of Aix-Marseille University - A*MIDEX, a French “Investissements d’Avenir” programme. D.H.J.O. was supported by NSERC (Canada). MRD acknowledges support from the EPSRC Centre for Doctoral Training in Topological Design (EP/S02297X/1).

* rodrigo.gutierrez-cuevas@espci.fr

† dodell@mcmaster.ca

‡ m.r.dennis@bham.ac.uk

§ miguel.alonso@fresnel.fr

- [1] J. J. Sakurai and J. J. Napolitano, *Modern Quantum Mechanics (2nd Edition)* (Pearson, 2010).
- [2] A. E. Siegman, *Lasers* (University Science Books, Sausal-

- ito, CA, 1986).
- [3] E. L. Ince, *Proceedings of the London Mathematical Society* **s2-23**, 56 (1925).
 - [4] F. M. Arscott, *Periodic Differential Equations* (Pergamon Press, 1964).
 - [5] B. P. Abbott *et al.* (LIGO Scientific Collaboration and Virgo Collaboration), *Phys. Rev. Lett.* **116**, 061102 (2016).
 - [6] L. Tao, A. Green, and P. Fulda, **102**, 122002 (2020).
 - [7] C. P. Boyer, E. G. Kalnins, and W. Miller, *J. Math. Phys.* **16**, 499 (1975).
 - [8] C. P. Boyer, E. G. Kalnins, and W. Miller, *J. Math. Phys.* **16**, 512 (1975).
 - [9] M. A. Bandres and J. C. Gutiérrez-Vega, *Opt. Lett.* **29**, 144 (2004).
 - [10] M. A. Bandres and J. C. Gutiérrez-Vega, *J. Opt. Soc. Am. A* **21**, 873 (2004).
 - [11] U. T. Schwarz, M. A. Bandres, and J. C. Gutiérrez-Vega, *Opt. Lett.* **29**, 1870 (2004).
 - [12] M. Krenn, R. Fickler, M. Huber, R. Lapkiewicz, W. Plick, S. Ramelow, and A. Zeilinger, *Phys. Rev. A* **87**, 012326 (2013).
 - [13] W. N. Plick, M. Krenn, R. Fickler, S. Ramelow, and A. Zeilinger, *Phys. Rev. A* **87**, 033806 (2013).
 - [14] M. Woerdemann, C. Alpmann, and C. Denz, *Appl. Phys. Lett.* **98**, 111101 (2011).
 - [15] G. J. Milburn, J. Corney, E. M. Wright, and D. F. Walls, *Phys. Rev. A* **55**, 4318 (1997).
 - [16] A. Smerzi, S. Fantoni, S. Giovanazzi, and S. R. Shenoy, *Phys. Rev. Lett.* **79**, 4950 (1997).
 - [17] S. Raghavan, A. Smerzi, S. Fantoni, and S. R. Shenoy, *Phys. Rev. A* **59**, 620 (1999).
 - [18] J. R. Anglin, P. Drummond, and A. Smerzi, *Phys. Rev. A* **64**, 063605 (2001).
 - [19] A. J. Leggett, *Rev Mod Phys* **73**, 307 (2001).
 - [20] R. Gati and M. K. Oberthaler, *J. Phys. B: At., Mol. Opt. Phys.* **40**, R61 (2007).
 - [21] E. M. Graefe and H. J. Korsch, *Phys. Rev. A* **76**, 032116 (2007).
 - [22] K. Sakmann, A. I. Streltsov, O. E. Alon, and L. S. Cederbaum, *Phys. Rev. Lett.* **103**, 220601 (2009).
 - [23] F. Nissen and J. Keeling, *Phys. Rev. A* **81**, 063628 (2010).
 - [24] M. Chuchem, K. Smith-Mannschott, M. Hiller, T. Kottos, A. Vardi, and D. Cohen, *Phys. Rev. A* **82**, 053617 (2010).
 - [25] D. H. J. O'Dell, *Phys. Rev. Lett.* **109**, 150406 (2012).
 - [26] E.-M. Graefe, H. J. Korsch, and M. P. Strzys, *J. Phys. A: Math. Theor.* **47**, 085304 (2014).
 - [27] K. Sukhatme, Y. Mukharsky, T. Chui, and D. Pearson, *Nature* **411**, 280 (2001).
 - [28] S. Backhaus, S. Pereverzev, R. W. Simmonds, A. Loshak, J. C. Davis, and R. E. Packard, *Nature* **392**, 687 (1998).
 - [29] F. S. Cataliotti, S. Burger, C. Fort, P. Maddaloni, F. Minardi, A. Trombettoni, A. Smerzi, and M. Inguscio, *Science* **293**, 843 (2001).
 - [30] M. Albiez, R. Gati, J. Fölling, S. Hunsmann, M. Cristiani, and M. K. Oberthaler, *Phys. Rev. Lett.* **95**, 010402 (2005).
 - [31] T. Schumm, S. Hofferberth, L. M. Andersson, S. Wildermuth, S. Groth, I. Bar-Joseph, J. Schmiedmayer, and P. Krüger, *Nat. Phys.* **1**, 57 (2005).
 - [32] S. Levy, E. Lahoud, I. Shomroni, and J. Steinhauer, *Nature* **449**, 579 (2007).
 - [33] L. J. LeBlanc, A. B. Bardonn, J. McKeever, M. H. T. Extavour, D. Jervis, J. H. Thywissen, F. Piazza, and A. Smerzi, *Phys. Rev. Lett.* **106**, 025302 (2011).
 - [34] C. Gerving, T. Hoang, B. Land, M. Anquez, C. Hamley, and M. Chapman, *Nat Commun* **3** (2012), 10.1038/ncomms2179.
 - [35] A. Trenkwalder, G. Spagnoli, G. Semeghini, S. Coop, M. Landini, P. Castilho, L. Pezzè, G. Modugno, M. Inguscio, A. Smerzi, and M. Fattori, *Nat. Phys.* **12**, 826 (2016).
 - [36] K. G. Lagoudakis, B. Pietka, M. Wouters, R. André, and B. Deveaud-Plédran, *Phys Rev Lett* **105**, 120403 (2010).
 - [37] M. Abbarchi, A. Amo, V. G. Sala, D. D. Solnyshkov, H. Flayac, L. Ferrier, I. Sagnes, E. Galopin, A. Lemaître, G. Malpuech, and J. Bloch, *Nat Phys* **9**, 275 (2013).
 - [38] R. Gutiérrez-Cuevas, S. A. Wadood, A. N. Vamivakas, and M. A. Alonso, *Phys. Rev. Lett.* **125**, 123903 (2020).
 - [39] M. R. Dennis and M. A. Alonso, *Phil. Trans. R. Soc. A* **375**, 20150441 (2017).
 - [40] R. Gutiérrez-Cuevas, M. R. Dennis, and M. A. Alonso, *J. Opt.* **21**, 084001 (2019).
 - [41] M. R. Dennis and M. A. Alonso, *J. Phys. Photonics* **1**, 025003 (2019).
 - [42] R. Gutiérrez-Cuevas and M. A. Alonso, *Opt Lett* **45**, 6759 (2020).
 - [43] See Supplemental Material at [URL will be inserted by publisher] for details about the Ince-Gauss modes, the derivation of the operator for the aberrated cavity and background information on the Bose-Hubbard dimer, which include Refs. [44-62].
 - [44] M. A. Alonso, *Adv. Opt. Photonics* **3**, 272 (2011).
 - [45] J. J. Healy, M. A. Kutay, H. M. Ozaktas, and J. T. Sheridan, *Linear canonical transforms: Theory and applications*, Vol. 198 (Springer, 2015).
 - [46] H. Lipkin, N. Meshkov, and A. Glick, *Nuclear Physics* **62**, 188 (1965).
 - [47] A. Das, K. Sengupta, D. Sen, and B. K. Chakrabarti, *Phys. Rev. B* **74**, 144423 (2006).
 - [48] J. W. Britton, B. C. Sawyer, A. C. Keith, C.-C. J. Wang, J. K. Freericks, H. Uys, M. J. Biercuk, and J. J. Bollinger, *Nature* **484**, 489 (2012).
 - [49] P. Richerme, Z.-X. Gong, A. Lee, C. Senko, J. Smith, M. Foss-Feig, S. Michalakakis, A. V. Gorshkov, and C. Monroe, *Nature* **511**, 198 (2014).
 - [50] J. G. Bohnet, B. C. Sawyer, J. W. Britton, M. L. Wall, A. M. Rey, M. Foss-Feig, and J. J. Bollinger, *Science* **352**, 1297 (2016).
 - [51] T. Zibold, E. Nicklas, C. Gross, and M. K. Oberthaler, *Phys. Rev. Lett.* **105**, 204101 (2010).
 - [52] J. Estève, C. Gross, A. Weller, S. Giovanazzi, and M. K. Oberthaler, *Nature* **455**, 1216 (2008).
 - [53] C. Gross, T. Zibold, E. Nicklas, J. Estève, and M. K. Oberthaler, *Nature* **464**, 1165 (2010).
 - [54] B. Juliá-Díaz, T. Zibold, M. K. Oberthaler, M. Melé-Messeguer, J. Martorell, and A. Polls, *Phys. Rev. A* **86**, 023615 (2012).
 - [55] H. L. Haroutyunyan and G. Nienhuis, *Physical Review A* **67**, 053611 (2003).
 - [56] G. J. Krahn and D. H. J. O'Dell, *Journal of Physics B: Atomic, Molecular and Optical Physics* **42**, 205501 (2009).
 - [57] H. Veksler and S. Fishman, *New J. Phys.* **17**, 053030 (2015).
 - [58] J. Mumford, E. Turner, D. W. L. Sprung, and D. H. J. O'Dell, *Phys. Rev. Lett.* **122**, 170402 (2019).

- [59] C. Chin, R. Grimm, P. Julienne, and E. Tiesinga, *Rev. Mod. Phys.* **82**, 1225 (2010).
- [60] L. Susskind and J. Glogower, *Physics* **1**, 49 (1964).
- [61] P. Carruthers and M. M. Nieto, *Rev. Mod. Phys.* **40**, 411 (1968).
- [62] D. T. Pegg and S. M. Barnett, *Phys. Rev. A* **39**, 1665 (1989).
- [63] M. A. Alonso and M. R. Dennis, *Optica* **4**, 476 (2017).
- [64] V. S. Shchesnovich and M. Trippenbach, *Phys. Rev. A* **78**, 023611 (2008).
- [65] D. Zor and K. G. Kay, *Phys. Rev. Lett.* **76**, 1990 (1996).
- [66] G. W. Forbes and M. A. Alonso, *J. Opt. Soc. Am. A* **18**, 1132 (2001).
- [67] M. A. Alonso and G. W. Forbes, *J. Opt. Soc. Am. A* **18**, 1146 (2001).
- [68] M. A. Alonso and G. W. Forbes, *Opt. Express* **10**, 728 (2002).
- [69] S. Pancharatnam, in *Proc. Ind. Acad. Sci.*, Vol. 44 (Springer, 1956) pp. 247–262.
- [70] M. V. Berry, *J. Mod. Opt.* **34**, 1401 (1987).
- [71] T. Malhotra, R. Gutiérrez-Cuevas, J. Hassett, M. R. Dennis, A. N. Vamivakas, and M. A. Alonso, *Phys. Rev. Lett.* **120**, 233602 (2018).
- [72] Y. Shen, X. Yang, D. Naidoo, X. Fu, and A. Forbes, *Optica* **7**, 820 (2020).
- [73] M. Jaffe, L. Palm, C. Baum, L. Taneja, and J. Simon, *Phys. Rev. Lett.* **104** (2021), 10.1103/physrev.104.013524.
- [74] N. Schine, A. Ryou, A. Gromov, A. Sommer, and J. Simon, *Nature* **534**, 671 (2016).
- [75] L. W. Clark, N. Schine, C. Baum, N. Jia, and J. Simon, *Nature* **582**, 41 (2020).
- [76] M. R. Dennis, *Opt. Lett.* **31**, 1325 (2006).
- [77] S. Lin Chao, *High order transverse modes in an astigmatic cavity*, Ph.D. thesis, University of Rochester (1974).
- [78] V. V. Ulyanov and O. B. Zaslavskii, *Phys. Rep.* **216**, 179 (1992).
- [79] J. Mumford, W. Kirkby, and D. H. J. O'Dell, *J. Phys. B: At., Mol. Opt. Phys.* **50**, 044005 (2017).
- [80] A. Vourdas, *Phys. Rev. A* **41**, 1653 (1990).
- [81] A. Luis and L. L. Sánchez-Soto, *Phys. Rev. A* **48**, 4702 (1993).
- [82] S. Longhi, *J. Phys. B: At., Mol. Opt. Phys.* **44**, 051001 (2011).
- [83] J. D. H. Morales, B. M. Rodríguez-Lara, and B. A. Malomed, *Opt. Lett.* **42**, 4402 (2017).
- [84] S. Becker, M. Mirahmadi, B. Schmidt, K. Schatz, and B. Friedrich, *Eur. Phys. J. D* **71**, 149 (2017).
- [85] M. Razavy, *Am. J. Phys.* **48**, 285 (1980).
- [86] G. Colombo, *Astron. J.* **71**, 891 (1966).
- [87] J. Henrard and C. Murigande, *Celestial Mech* **40**, 345 (1987).
- [88] C. K. Law, H. Pu, and N. P. Bigelow, *Phys Rev Lett* **81**, 5257 (1998).
- [89] B. Evrard, A. Qu, J. Dalibard, and F. Gerbier, *Phys Rev Lett* **126**, 063401 (2021).
- [90] W. Kirkby, Y. Yee, K. Shi, and D. H. J. O'Dell, *Phys. Rev. Research* **4**, 013105 (2022).